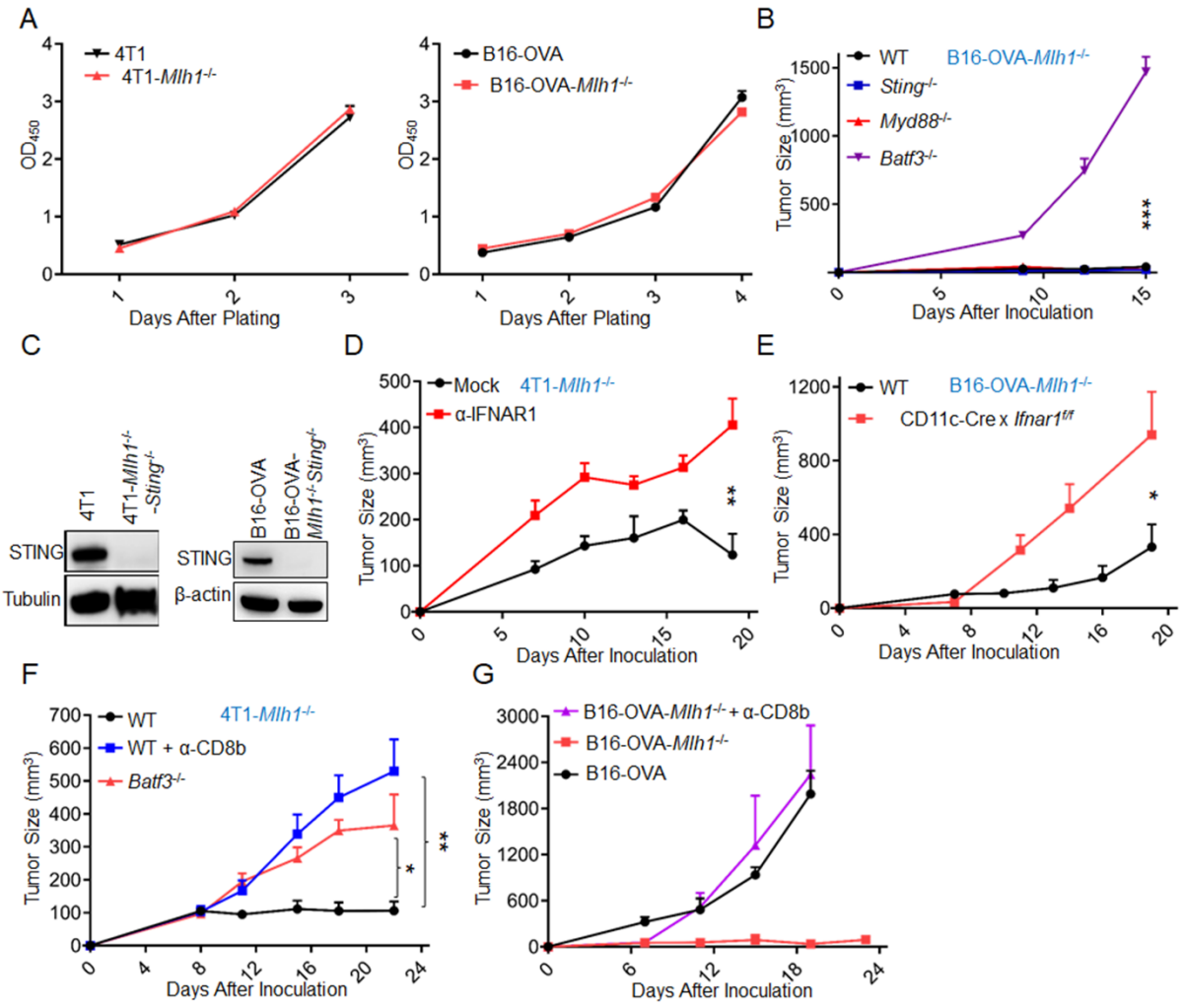
A
4T1
4T1-Mlh1-/-
OD450
Days After Plating
B16-OVA
B16-OVA-Mlh1-/-
Days After Plating
B
WT
B16-OVA-Mlh1-/-
Sting-/-
Myd88-/-
Batf3-/-
Tumor Size (mm3)
***
Days After Inoculation
C
4T1
4T1-Mlh1-/--Sting-/-
STING
Tubulin
B16-OVA
B16-OVA-Mlh1-/-Sting-/-
STING
β-actin
D
Mock
4T1-Mlh1-/-
α-IFNAR1
Tumor Size (mm3)
**
Days After Inoculation
E
WT
B16-OVA-Mlh1-/-
CD11c-Cre x Ifnar1f/f
Tumor Size (mm3)
*
Days After Inoculation
F
WT
4T1-Mlh1-/-
WT + α-CD8b
Batf3-/-
Tumor Size (mm3)
*
**
Days After Inoculation
G
B16-OVA-Mlh1-/- + α-CD8b
B16-OVA-Mlh1-/-
B16-OVA
Tumor Size (mm3)
Days After Inoculation

Figure S1. Host IFNAR1 pathway is essential for dMLH1 tumor progression, Related to Figure 1

(A) 4T1 and 4T1-*Mlh1*$^{-/-}$ cells, B16-OVA and B16-OVA-*Mlh1*$^{-/-}$ cells, were inoculated into 96-well plate and cultured for different days. Cell proliferation rate was determined by the Cell Counting Kit-8.

(B) B16-OVA cells (5×10^5 cells/mouse) with dMLH1 (D166) were subcutaneously inoculated into WT, *MyD88*$^{-/-}$, *Sting*$^{-/-}$ and *Batf3*$^{-/-}$ mice (n=5).

(C) *Sting* were knocked out in 4T1-*Mlh1*$^{-/-}$ cells and B16-OVA-*Mlh1*$^{-/-}$ cells.

(D) 4T1 cells with dMLH1 (D166) were inoculated into WT BALB/C mice (n=5), with or without 200 μg of anti-IFNAR1 mAb at days 0, 3 and 6 after inoculation.

(E) B16-OVA cells with dMLH1 (D170) were inoculated into WT and CD11c-Cre; *Ifnar1*$^{f/f}$ mice (n=4). (F) 4T1 cells with dMLH1 (D165) were inoculated into *Batf3*$^{-/-}$ mice (n=5) or WT BALB/C mice (n=5) with or without 200 μg of anti-CD8b mAb at days 0, 3, 7, and 10 after inoculation.

(G) B16-OVA and B16-OVA-*Mlh1*$^{-/-}$ cells were inoculated into WT BALB/C mice (n=5-7) at 5×10^5 cells/mouse. Mice were depleted of T cells at day 0 and 5 after inoculation with 200 μg/mouse anti-CD8b mAb. The differences of tumor size at day 19 between B16-OVA and T-cell depleted B16-OVA-*Mlh1*$^{-/-}$ group were not significant (p=0.7005).

Unpaired t test was used to determine significance.

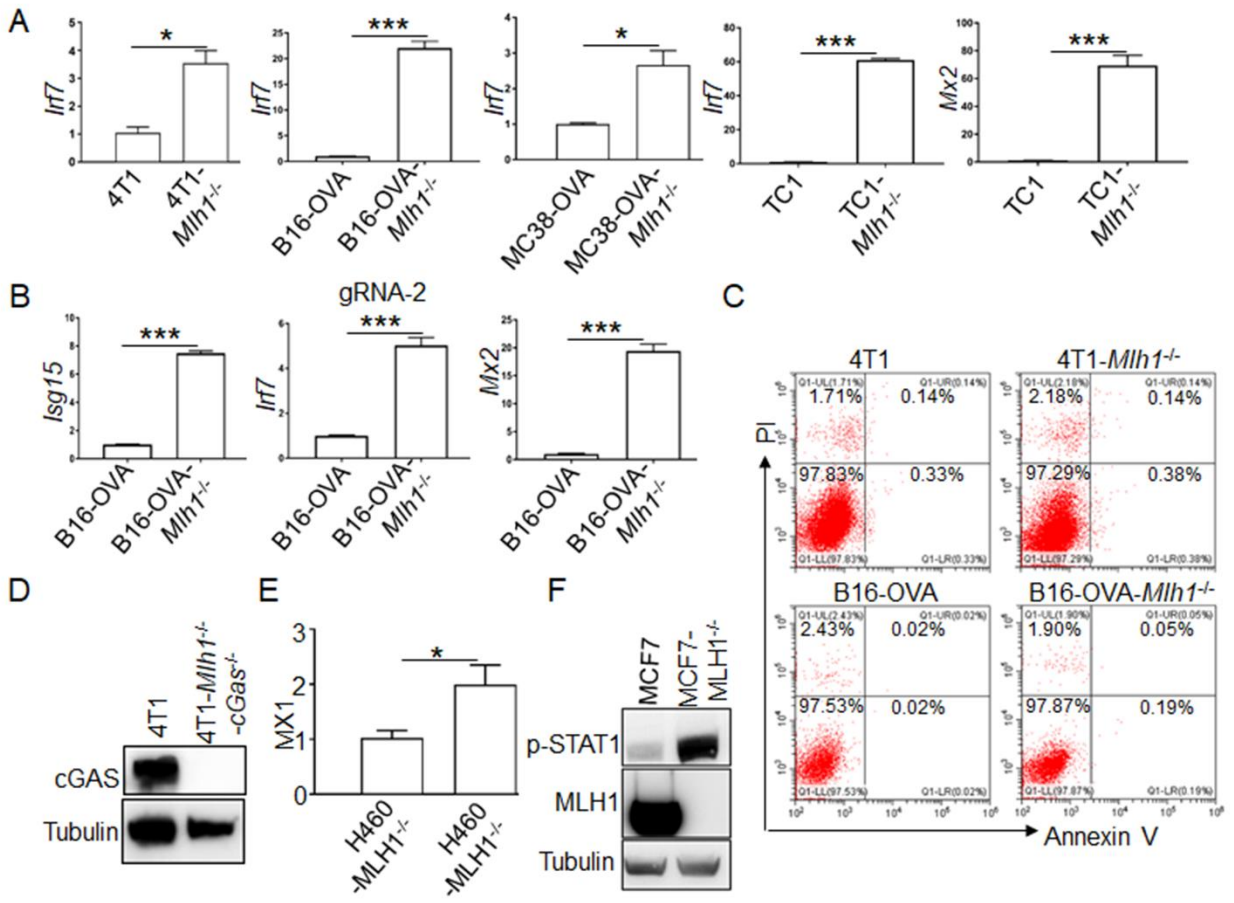

Figure S2. Activation of type I IFN signal pathway in dMLH1 tumor cell lines, Related to Figure 2

(A**)** ISGs expression at mRNA level were determined in different mouse tumor cell lines.

(B) *Mlh1* gene was knocked out in B16-OVA cells with another set of gRNAs, and ISGs expression were determined.

(C) 4T1 and 4T1-*Mlh1*$^{-/-}$ cells, B16-OVA and B16-OVA-*Mlh1*$^{-/-}$ cells, were cultured in vitro for 2 days, then digested and stained with propidium iodide (PI) and Annexin V.

(D) *cGAS* was knocked out in 4T1-*Mlh1*$^{-/-}$ cells, western blots data were shown.

(E and F) MX1 expression and phosphorylation of STAT1 at Y701 were determined in human cancer cell lines H460 and MCF7.

Unpaired t test was used to determine significance.

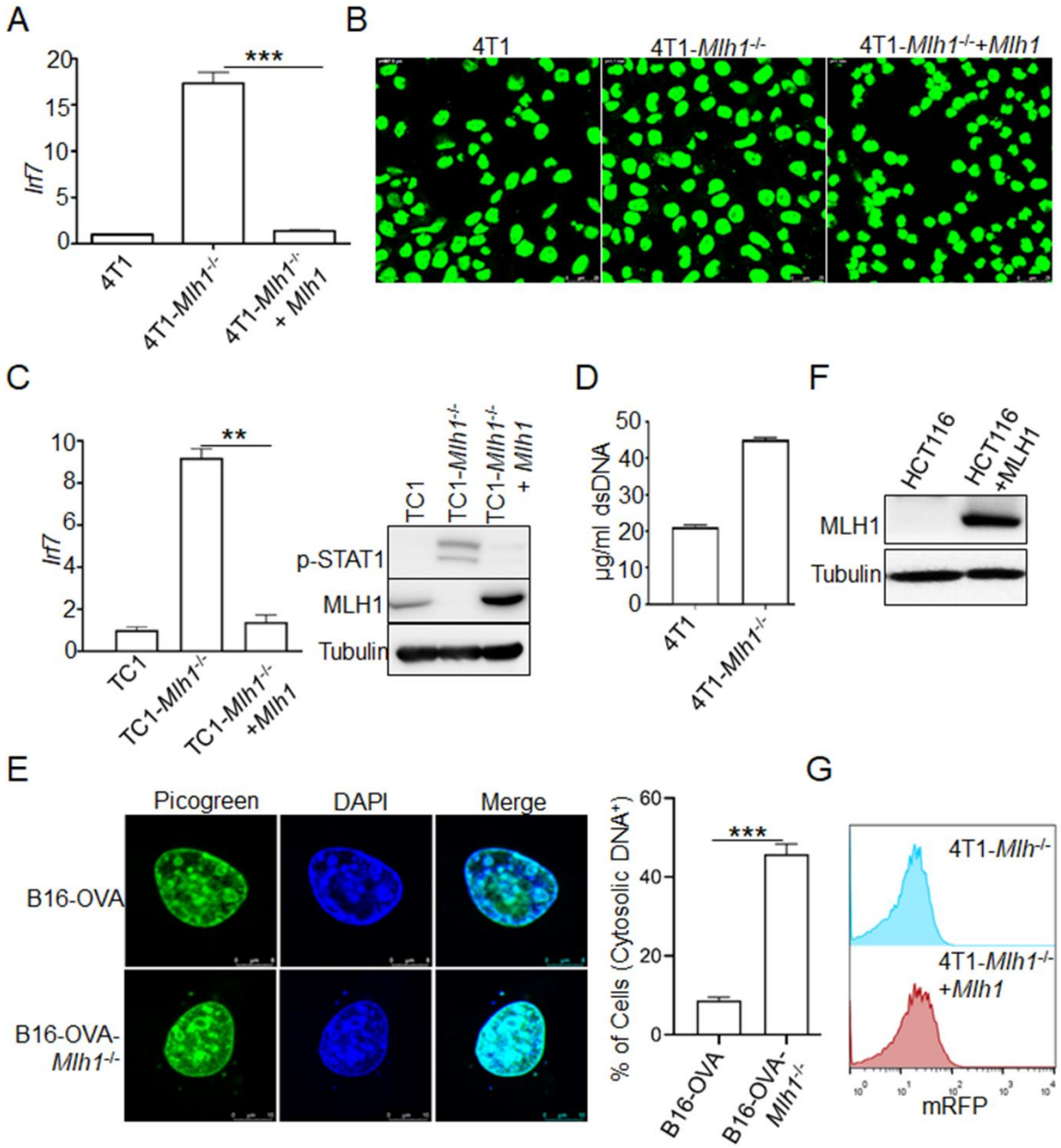
A
Irf7
20
15
10
5
0
***
4T1
4T1-Mlh1-/-
4T1-Mlh1-/- + Mlh1
B
4T1
4T1-Mlh1-/-
4T1-Mlh1-/-+Mlh1
C
Irf7
10
8
6
4
2
0
**
TC1
TC1-Mlh1-/-
TC1-Mlh1-/- +Mlh1
p-STAT1
MLH1
Tubulin
D
µg/ml dsDNA
50
40
30
20
10
0
4T1
4T1-Mlh1-/-
F
HCT116
HCT116 +MLH1
MLH1
Tubulin
E
Picogreen
DAPI
Merge
B16-OVA
B16-OVA-Mlh1-/-
% of Cells (Cytosolic DNA+)
60
40
20
0
***
B16-OVA
B16-OVA-Mlh1-/-
G
4T1-Mlh-/-
4T1-Mlh1-/- +Mlh1
mRFP

Figure S3. MLH1 regulates accumulation of cytosolic DNA in tumor cells and immunotherapy in vivo, Related to Figure 3

(A**)** *Irf7* expression at mRNA level was determined in MLH1-rescued cells.

(B) dsDNA was stained by PicoGreen reagents in MLH1-rescued cells.

(C**)** *Irf7* and phosphorylation of STAT1 at Y701 expression at mRNA level were determined in MLH1-rescued cells.

(D**)** Cytosolic fractionation was isolated by ultracentrifugation, and dsDNA was absolutely quantified by PicoGreen dsDNA quantification fluorescence method.

(E) dsDNA in B16-OVA cells was stained using PicoGreen reagents. Extra-nuclear dsDNA was counted, and statistical data are shown.

(F) MLH1 expression is shown in HCT116 cells.

(G) 4T1-*Mlh1*$^{-/-}$ cells were infected with lentivirus expressing either MLH1-IRES-mRFP or mRFP alone. mRFP positive cells were sorted, and mRFP level was shown by FACS.

Unpaired t test was used to determine significance.

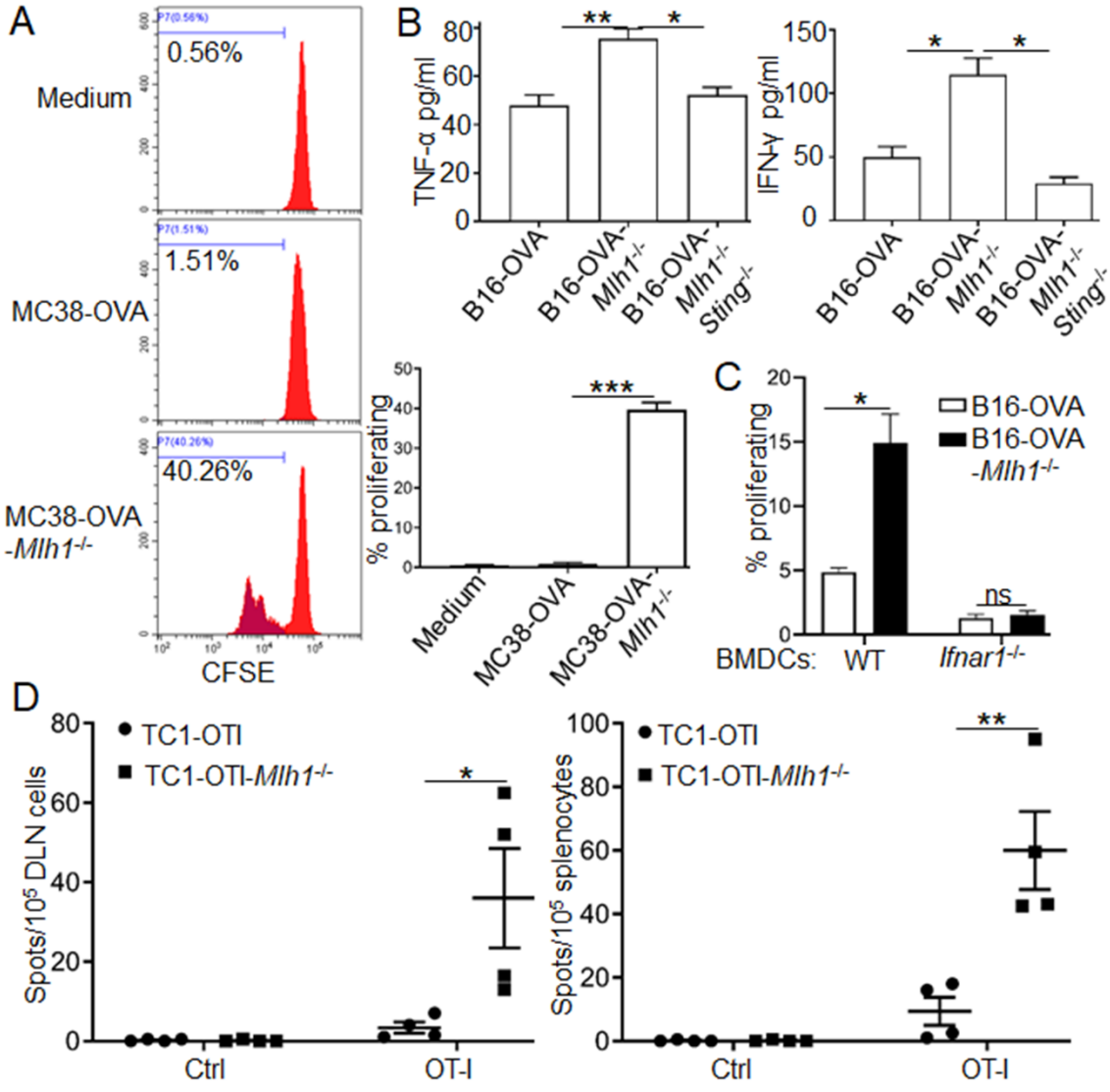
A
Medium
0.56%
MC38-OVA
1.51%
MC38-OVA
-Mlh1-/-
40.26%
CFSE
B
TNF-α pg/ml
IFN-γ pg/ml
B16-OVA
B16-OVA-Mlh1-/-
B16-OVA-Mlh1-/-Sting-/-
% proliferating
Medium
MC38-OVA
MC38-OVA-Mlh1-/-
C
% proliferating
B16-OVA
B16-OVA -Mlh1-/-
ns
BMDCs: WT
Ifnar1-/-
D
TC1-OTI
TC1-OTI-Mlh1-/-
Spots/10^5 DLN cells
Spots/10^5 splenocytes
Ctrl
OT-I

Figure S4. T cells respond better to specific antigen in dMLH1 tumor cells, Related to Figure 4

(A**)** Like in Figure 4A, here the ratio of DC: T is 1:20.
(B) Like in Figure 4A. After over-night co-culture with indicated tumor cells, BMDCs were isolated and added into a 96-well plate together with purified CFSE-labelled OT-I T cells for 2 days, then IFN-γ and TNF-α in supernatant were quantified by Cytometric Bead Array. Statistical data are shown.
(C) BMDCs (WT mice and *Ifnar1*-deficient mice) pre-educated with B16-OVA cells and B16-OVA-*Mlh1*$^{-/-}$ cells were purified and co-cultured with purified OT-I T cells, then T-cell proliferation was determined 3 days later by FACS.
(D) TC1-OTI cells were inoculated into WT C57BL/6 mice (n=4). One week later, cells from spleen and draining lymph nodes were isolated and re-stimulated by OT-I peptide or control SIY peptide in vitro, T cell responses were determined by IFN-γ ELISPOT assay. Statistical data are shown.
Unpaired t test was used to determine significance of differences.

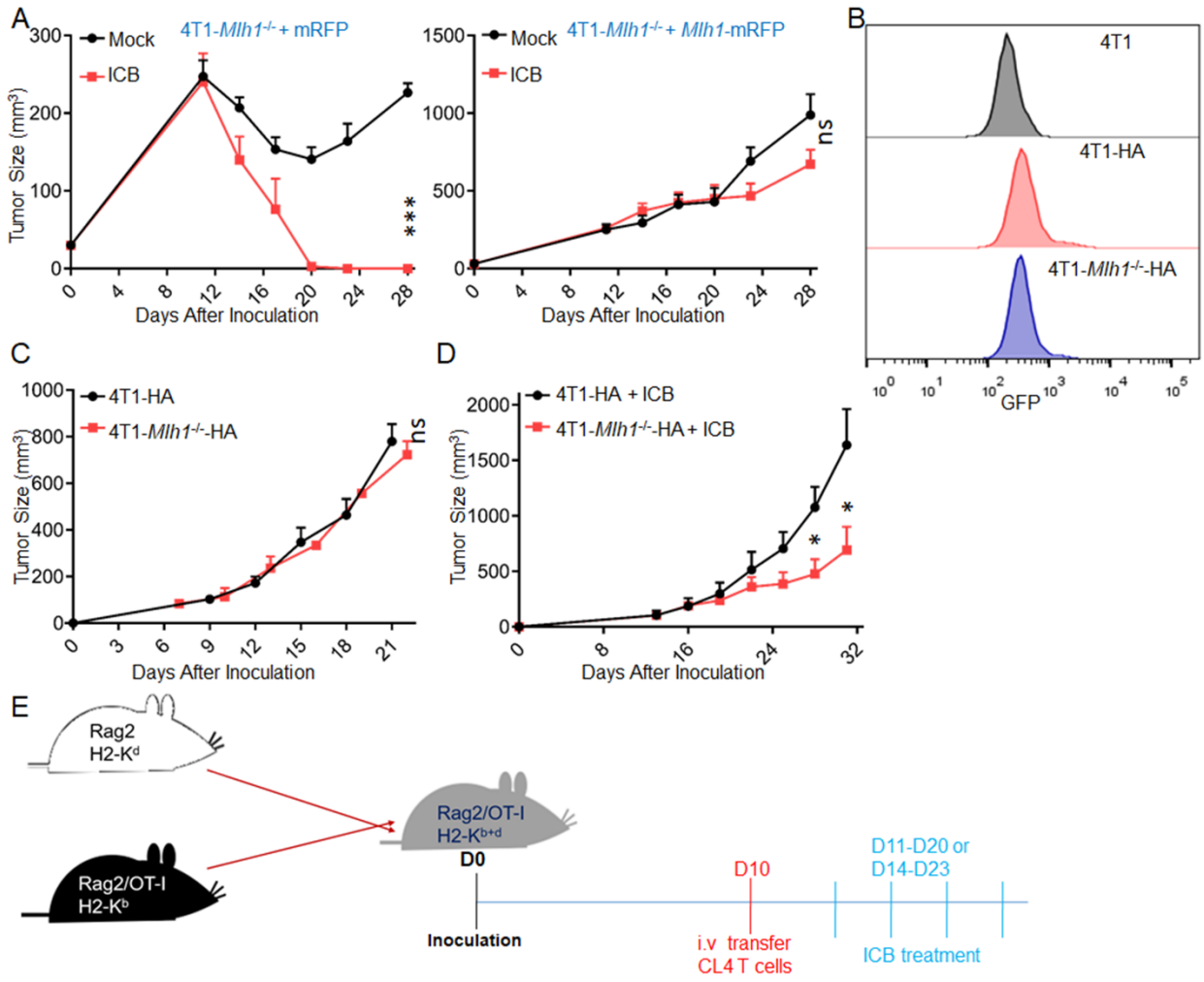

Figure S5. 4T1-HA model construction, Related to Figure 5

(A) Fragmented tumor tissues derived from 4T1-*Mlh1*$^{-/-}$ and 4T1-*Mlh1*$^{-/-}$+MLH1 cells in Rag1 mice were implanted into WT mice (n=4-5), and treated with ICB drugs at day 11, 14 and 17. Tumor curves are shown. ***p<0.0001 between the two groups in 4T1-MLH1$^{-/-}$ model; ns, P=0.0866 between the groups in 4T1-*Mlh1*$^{-/-}$+MLH1 model.

(B) 4T1 and 4T1-*Mlh1*$^{-/-}$ cells were infected by lentivirus expressing HA-GFP fusion protein. GFP positive cells were sorted, and GFP level was shown by FACS.

(C) Cell lines in (B) were inoculated into F1 mice of Rag2×Rag2/OT-I to compare in vivo growth without treatment. No significant differences were found.

(D) 4T1-HA and 4T1-HA-*Mlh1*$^{-/-}$ cells were inoculated into F1 mice (n=5-7) of Rag2× Rag2/OT-I mice, followed by CL4 T-cell transfer at day 14 and ICB treatment at day 18, 21 and 24. *P=0.0364 at day 28, *P=0.0419 at day 31 between the two groups.

(E) Schematic diagram showing ICB treatment in 4T1-HA model.

Unpaired t test was used to determine significance of differences.

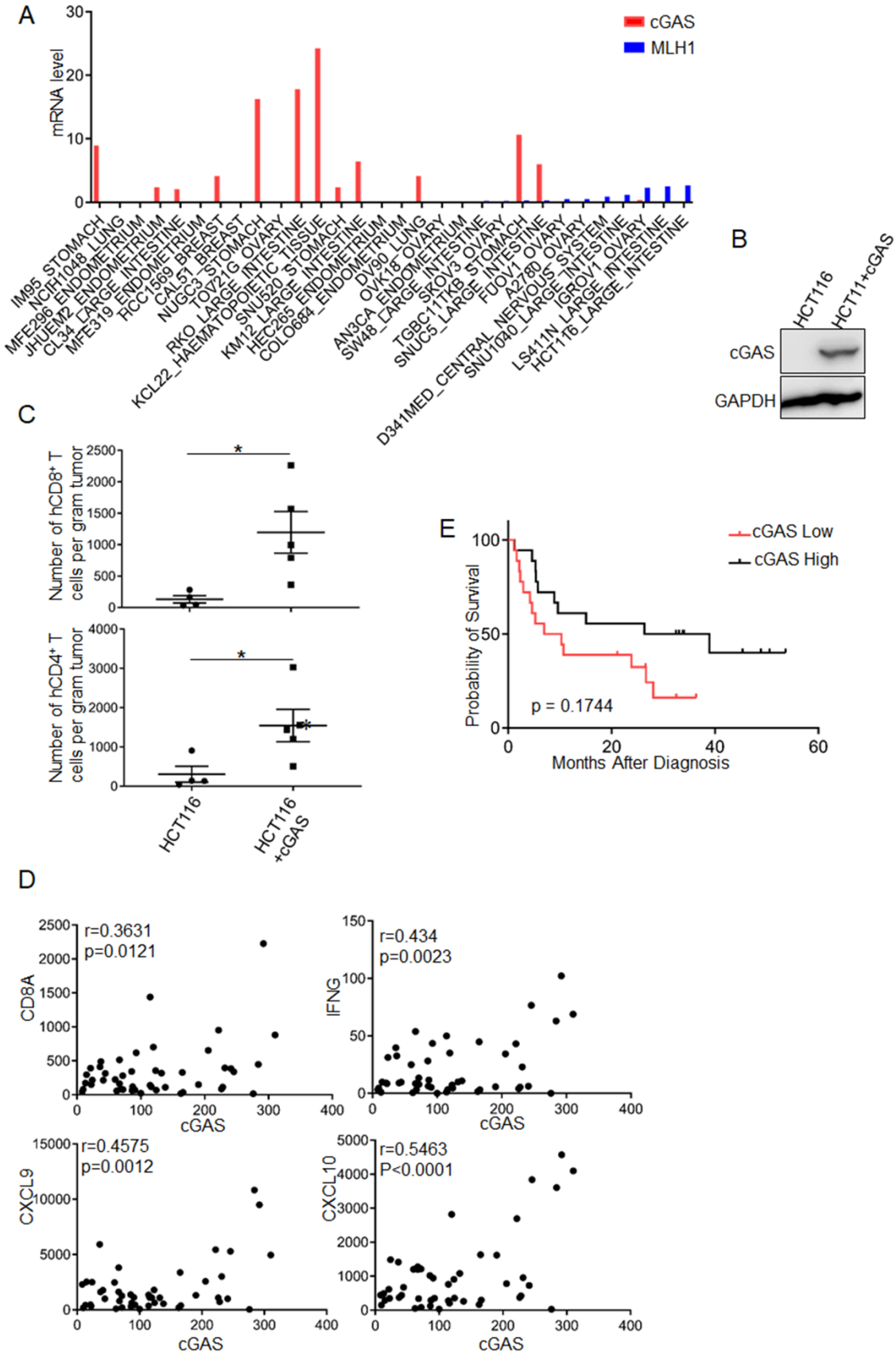
A
cGAS
MLH1
mRNA level
30
20
10
0
IM95_STOMACH
NCIH1048_LUNG
MFE296_ENDOMETRIUM
JHUEM2_ENDOMETRIUM
CL34_LARGE_INTESTINE
MFE319_ENDOMETRIUM
RCC1569_BREAST
CAL51_BREAST
NUGC3_STOMACH
TOV21G_OVARY
RKO_LARGE_INTESTINE
KCL22_HAEMATOPOIETIC_TISSUE
KM12_LARGE_INTESTINE
SNU520_STOMACH
HEC265_ENDOMETRIUM
COLO684_ENDOMETRIUM
DV90_LUNG
OVK18_OVARY
AN3CA_ENDOMETRIUM
SW48_LARGE_INTESTINE
SROV3_OVARY
TGBC11TKB_STOMACH
SNUC5_LARGE_INTESTINE
D341MED_CENTRAL_NERVOUS_SYSTEM
SNU1040_LARGE_INTESTINE
A2780_OVARY
FUOV1_OVARY
IGROV1_OVARY
LS411N_LARGE_INTESTINE
HCT116_LARGE_INTESTINE
B
HCT116
HCT11+cGAS
cGAS
GAPDH
C
Number of hCD8+ T cells per gram tumor
2500
2000
1500
1000
500
0
*
Number of hCD4+ T cells per gram tumor
4000
3000
2000
1000
0
*
HCT116
HCT116 +cGAS
E
cGAS Low
cGAS High
Probability of Survival
100
50
0
p = 0.1744
0
20
40
60
Months After Diagnosis
D
CD8A
r=0.3631
p=0.0121
2500
2000
1500
1000
500
0
0
100
200
300
400
cGAS
IFNG
r=0.434
p=0.0023
150
100
50
0
0
100
200
300
400
cGAS
CXCL9
r=0.4575
p=0.0012
15000
10000
5000
0
0
100
200
300
400
cGAS
CXCL10
r=0.5463
P<0.0001
5000
4000
3000
2000
1000
0
0
100
200
300
400
cGAS

Figure S6. cGAS expression correlates with tumor-infiltration of $CD8^+$ T cells in MSI tumors, Related to Figure 6

(A) The mRNA level of cGAS is shown among a list of human dMLH1 cancer cell lines.
(B) Human cGAS expression is shown in HCT116 cells.
(C) HCT116 and HCT116+cGAS cells were inoculated into human immune cell chimeric mice (n=4-5). One week later, tumor-infiltrated $CD8^+$ and $CD4^+$ T cells were detected by FACS.
(D) Correlation analysis of cGAS expression level with the expression level of CD8A, IFNG, CXCL9 and CXCL10, respectively, in MSI-H human colorectal adenocarcinoma (see Table S2 for patient information).
(E) The curves between cGAS expression with overall survival in melanoma patients (n=17-18) treated with ipilimumab are shown (see Table S3 for patient information).
Unpaired t test was used to determine significance of differences in C. The log-rank test for E. Pearson correlation coefficient (two-tailed) was performed to determine the correlation in D.